

MOTR: End-to-End Multiple-Object Tracking with TFormer

Fangao Zeng* Bin Dong* Tiancai Wang* Cheng Chen
 Xiangyu Zhang Yichen Wei

MEGVII Technology

{zengfangao, dongbin, wangtiancai, chencheng03, zhangxiangyu, weiyichen}@megvii.com

Abstract

The key challenge in multiple-object tracking (MOT) task is temporal modeling of the object under track. Existing tracking-by-detection methods adopt simple heuristics, such as spatial or appearance similarity. Such methods, in spite of their commonality, are overly simple and insufficient to model complex variations, such as tracking through occlusion. Inherently, existing methods lack the ability to learn temporal variations from data.

In this paper, we present MOTR, the first fully end-to-end multiple-object tracking framework. It learns to model the long-range temporal variation of the objects. It performs temporal association implicitly and avoids previous explicit heuristics. Built on Transformer and DETR, MOTR introduces the concept of “track query”. Each track query models the entire track of an object. It is transferred and updated frame-by-frame to perform object detection and tracking, in a seamless manner. Temporal aggregation network combined with multi-frame training is proposed to model the long-range temporal relation. Experimental results show that MOTR achieves state-of-the-art performance. Code is available at <https://github.com/megvii-model/MOTR>.

1. Introduction

Multiple-object tracking (MOT) is a class of visual object detection, where the task is not only localize all targets in each frame but also predict the moving trajectories of those objects in the whole video sequences. The problem is challenging since objects in each frame maybe occluded in pool environment and the tracker developed may suffer from long-term and low-rate tracking. These complex and diverse tracking scenarios impose significant challenges when designing a MOT solution.

*Equal contribution. This work is supported by The National Key Research and Development Program of China (No.2017YFA0700800) and Beijing Academy of Artificial Intelligence (BAAI).

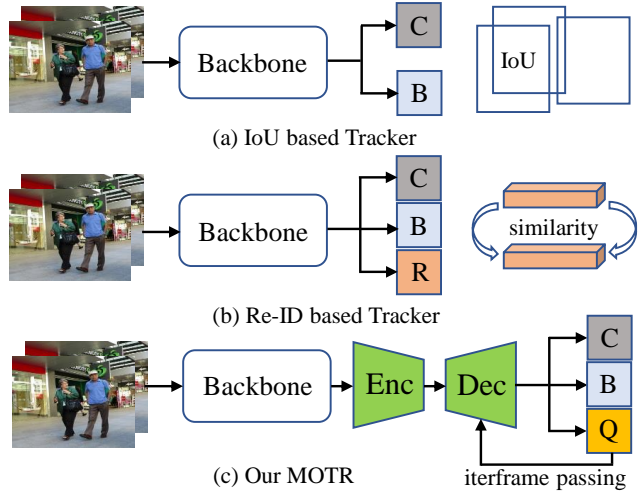


Figure 1. (a) IoU based object trackers associate the temporal tracks by the overlap of bounding boxes predicted from adjacent frames. (b) Re-ID based object trackers predict the Re-ID feature embeddings parallel with the detection branch and associate the tracks by calculating the feature similarity. (c) Parallel with the detection branch, our MOTR predicts a track query set, in which each track query is responsible to predict the entire track of an object. The query set is recurrently input to the decoder to produce the tracking predictions for the current frame. ‘C’: classification. ‘B’: box regression. ‘R’: Re-ID embedding. ‘Q’: track query.

Most existing approaches [39, 44, 1, 45] follow the tracking-by-detection paradigm. It predicts the tracking trajectories by decomposing the problem into two parts: object localization and temporal association. For object localization, an object detector [27, 46, 26] is employed to detect objects frame by frame. For temporal association, existing methods either use spatial similarity, that is interaction of union (IoU) based, or appearance similarity, that is re-identification (Re-ID) based. For IoU based methods [45, 3, 4], IoU matrix of detected boxes from two adjacent frames is calculated and boxes whose overlap is higher than the given threshold are associated with the same identity (see Fig. 1(a)). Similarly, Re-ID based approaches [1, 41] compute the feature similarity from adjacent frames and as-

sociate the object pairs with high similarity. Further, some recent works [39, 44] have attempted joint training of object detection and Re-ID feature learning (see Fig. 1(b)).

Above temporal association methods are heuristic and overly simple. It’s hard for them to model the complexity of variation in spatial and appearance of an object in a long time interval. Inherently, they lack the mechanism to model the temporal variation from data, which is against the spirit of “end-to-end learning of everything” in the current deep learning era. While they work mostly fine under common scenarios, they are not robust to challenging scenarios and easily fail once irregularity is encountered, which however, is the key challenge in MOT problem. For instance, it is pretty hard to distinguish the tracks by the IoU matching in occluded area. Beside the occluded scene, some extreme cases, like strong light, dark night and object deformation, are fatal for those Re-ID based trackers. In this work, we look into an alternative approach that addresses these shortcomings by building an end-to-end tracking framework without any association processes.

Recently, DETR [6, 47] is proposed for end-to-end learning of object detection. It proposes the concept of “object query”, which is an explicit and decoupled representation of object. This representation eases learning in the framework of transformer. Motivated by DETR’s great success, this work extends the “object query” concept to model object tracking, called *track query* in this work. Each track query is responsible to predict an entire track of an object. As shown in Fig. 1(c), parallel with the classification and box regression branches, MOTR predicts the track query set at each frame. The track query set is input to the decoder network to directly produce the tracking predictions for the current frame and the updated track query (output by the decoder). The updated track query is further passed to the decoder for the next frame. Such query passing and prediction process is repeated frame-by-frame for the whole video sequences, called *continuous query passing*. Since each track query follows the same object all the time once the query is matched by one object, continuous query passing can naturally remove the temporal associations and some hand-craft operations, like NMS. To model the long-range temporal relation, we further introduce multi-frame training and the temporal aggregation network (TAN). TAN builds up a query memory bank to collect the queries in history that correspond to the tracked objects. The track query of current frame will interact with each query in the memory bank through the multi-head attention.

Our proposed MOTR is simple and effective. It is the *first* strictly end-to-end framework for MOT task. There is no temporal association process or hand-craft operations, thanks to temporal modeling capability of track query learnt via the multi-frame temporal aggregation. On the contrary, concurrent Transformer-based works [35, 22] are not fully

end-to-end as they still employ IoU-matching or Tracking NMS. The experimental results on MOT16 and MOT17 datasets [24] show that MOTR achieves state-of-the-art performance, at much lower algorithm complexity, compared to previous MOT methods. Especially, MOTR greatly reduces the ID Switches and improve the IDF1 metric, achieving promising tracking performance.

To summarize, our contributions are:

- We propose a fully end-to-end framework for multiple-object tracking. Different from IoU based or Re-ID based approaches that require explicit association process, our method directly produces tracking predictions without any explicit associations.
- We introduce the concept of *track query* and the *contiguous query passing* mechanism. Modeling of the long-range temporal variation of the object is learned from data with this mechanism.
- Temporal aggregation network combined with multi-frame training is further proposed to help model the long-range temporal relation. It allows our MOTR efficiently reduce ID Switches, caused by lack of temporal information.

2. Related Work

Transformer-based Architectures: Transformer [37] is first introduced to aggregate information from the entire input sequence for machine translation. It mainly involves self-attention and cross-attention mechanisms. Since that, transformer is gradually introduced to many problems such as speech processing [18, 7] and computer vision [38, 5]. Recently, DETR [6] combines convolutional neural network (CNN) with Transformer and Hungary matching to perform end-to-end object detection. FPT [43] employs feature pyramid transformer architecture to fuse and interact multi-scale features for object detection. ViT [10] uses transformer architecture for image classification task by dividing the image into 16x16 patches as the input of transformer after linear projection. To speed up the convergence of DETR, Deformable DETR [47] introduces deformable Transformer to construct deformable attention module inserted in the encoder and decoder. IPT [8] proposes a transformer-based pretrained network for low-level image processing.

Multiple-Object Tracking: To date, the dominant frameworks for MOT mainly follow the tracking-by-detection paradigm [2, 16, 31, 33, 41]. Those approaches firstly employ object detectors to localize all objects in the each frame and then perform temporal association among adjacent frames to produce final tracking results. SORT[2] tracks bounding boxes by combining Kalman Filter[40] and Hungarian algorithm[15] with IoU distance. DeepSORT[41] and Tracktor[1] introduce the extra cosine distance and

compute it based on the extracted appearance features for temporal association. Track-RCNN[34], JDE[39] and FairMOT[44] further add a Re-ID branch on top of object detector in a joint training framework, incorporating object detection and Re-ID feature learning.

Based on DETR, our concurrent works, TransTrack [35] and TrackFormer [22] also develop the Transformer-based frameworks for MOT. However, TransTrack is simply a unified framework that jointly trains the detection and tracking. However, the tracks are still associated by the IoU matching. Whereas our MOTR shares some similarities with TrackFormer, some major differences include: 1) Our MOTR is a fully end-to-end framework for MOT and removes the need for NMS, used in TrackFormer. 2) Temporal aggregation network combined with multi-frame training is proposed to model the long-range temporal relation.

3. Methods

3.1. Revisiting Deformable DETR

Recently, DETR [6] succeed in object detection by adopting the Transformer. In DETR, the object queries, a fixed number of learned positional embeddings, represent the proposals of some possible instances. One object query only corresponds to one object with the employment of bipartite matching. Considering the high complexity and slow convergence problems existing in DETR, Deformable DETR [47] simply replaces the self-attention in Transformer with multi-scale deformable attention. To show how the object queries interact with the features through the decoder, we reformulate the decoder of Deformable DETR.

Decoder: Let $q \in R^C$ denotes a set of object queries and $f \in R^C$ represents the feature map from the encoder network, where C is the feature dimension. Then, the decoder process can be formulated as:

$$q^k = G_{ca}(G_{sa}(q^{k-1}), f) \quad (1)$$

where $k \in 1, \dots, K$ and K is the total number of decoder layers. q^k are the output queries of the k^{th} decoder layer. G_{sa} is the self-attention as that in DETR and G_{ca} denotes the multi-scale deformable attention.

3.2. MOTR

In MOTR, we introduce the track query and continuous query passing to perform the tracking predictions in a fully end-to-end manner. The temporal aggregation network is further proposed to enhance the temporal information of multiple frames.

3.2.1 End-to-End Track Query Passing

Detection Query vs Track Query: Object (detection) query introduced in DETR is not responsible to predict for

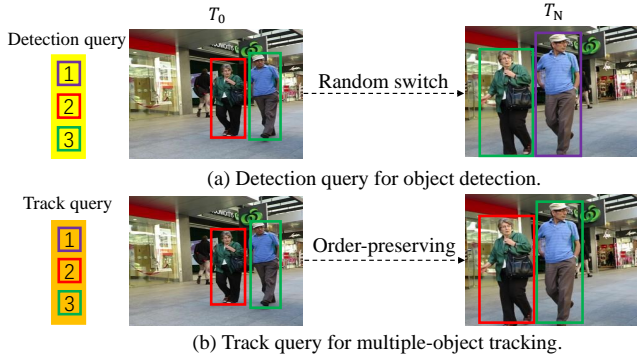


Figure 2. Comparison of track query, employed in MOTR, with the detection query in object detection.(a) detection query for detection: the query is related to the position the object locates. When the positions of object changes, the query identity will randomly switch. (b) track query for multiple-object tracking: Once the track query is matches with one object, the query identity of the object will not switch until the object disappears.

specific object. So one object query may predict different objects as the input image varies. When employing the DETR detector on the examples in MOT dataset, as shown in Fig. 2(a), the same detection query (the green object query) predicts two different objects at two different frames. Therefore, it is hard to associate the detection predictions as tracks by the identity of object query.

As a remedy, we extend the object query to model the object tracking, namely track query. In our design, each track query is responsible to predict an entire track of an object. Once the track query is matched with one object at a frame, it will always predict for the object until the object disappears (see Fig. 2(b)). Thus, all prediction results from the same track query naturally form the track of the object without explicit associations. The order-preserving of track query is learned by the target-determined supervision of the track queries. To deal with the new objects appearing at current frame, we further introduce the empty query. For more details about the supervision, please refer to the Sec. 3.2.3.

Continuous Query Passing: Based on the track query introduced above, we propose the continuous query passing mechanism. In this mechanism, the track query is transferred frame-by-frame to iteratively update the representation and localization of the object with which the query is matched. Here, we present MOTR, a fully end-to-end MOT framework through the continuous query passing. In MOTR, the modeling of temporal variance of objects is implicitly learned by the decoder’s multi-head attention instead of explicit association. The overall architecture of MOTR is shown in Fig. 3. Video sequences are first input to the convolutional neural network (CNN) (e.g. ResNet-50 [12]) and the encoder in Deformable DETR [47] to extract the basic feature list $f = \{f_0, f_1, \dots, f_N\}$. For the T_0 frame, the basic feature f_0 together with the empty query set q_e is input to the decoder network to localize all initial objects

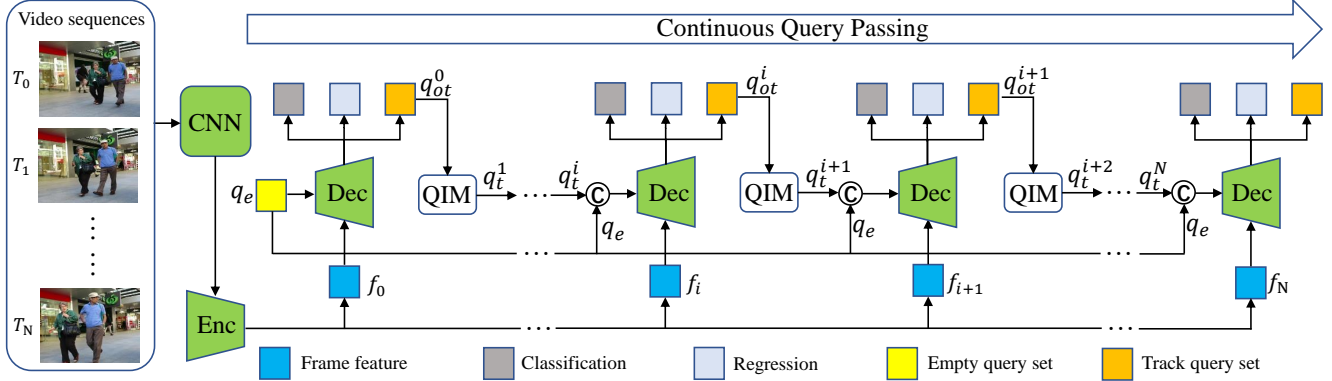


Figure 3. Overall architecture of the proposed MOTR. Multi-frame video sequences are input to the convolutional backbone network (e.g. ResNet-50) and the encoder network to extract multi-frame basic feature list $f = \{f_0, f_1, \dots, f_N\}$. For the initial T_0 frame, the basic feature f_0 together with the empty query q_e (yellow box) is injected to the decoder network to localize the initial objects and generate the initial track query for the T_1 frame. For the T_i frames, the original track query q_{ot}^i predicted by the previous frame is updated by the empty query through the query interaction module (QIM) to generate the track query q_t^i for current frame. Continuous query passing is performed to transfer the track query within the whole video sequences.

and generate the original track query set q_{ot}^1 as well. The original track query set q_{ot}^0 passes through the query interaction module (QIM) to generate the track query set q_t^1 for the T_1 frame. For the T_i frame, where $i \in [1, N]$, the track query set q_t^i generated by the QIM from the T_{i-1} frame and the empty query set q_e will be concatenated. The concatenated query set together with the basic feature f_i is input to the shared decoder to directly generate the predictions for the current frame as well as the original track query set q_{ot}^{i+1} for the T_{i+1} frame. Such process is repeated for the whole video sequences.

3.2.2 Query Interaction Module

In this section, we describe the query interaction module (QIM) in detail. QIM mainly includes object entrance and exit mechanism and the temporal aggregation network.

Object Entrance and Exit: As mentioned in Sec. 3.2.1, each track query represents an entire track. However, some objects in the video sequences tend to appear or disappear at intermediate frames. Therefore, MOTR is required to output a sequence of bounding boxes $\{box_i, \dots, box_j\}$ assuming that one object appears at T_i frame and disappears at T_j frame. Here, we introduce how to deal with the cases of object entrance and object exit in MOTR.

During training phase, the learning of track query can be achieved based on the supervision of those ground-truths (GTs) matched by the bipartite matching. While for the inference, we use the track scores predicted to determine when a track appears and disappears. As shown in Fig. 4, for the T_i frame, the track query set q_t^i generated by QIM from the T_{i-1} frame and the empty query set q_e are concatenated together. The concatenated query set is then input to the decoder and produce the original track query set q_{ot}^i with

track scores. The original track query q_{ot}^i is then split into two query sets: $q_{en}^i = q_{ot}^i[:d_e]$ and $q_{ce}^i = q_{ot}^i[d_e:]$, where d_e is the number of queries in empty query set q_e . q_{en}^i contains entrance objects while q_{ce}^i includes both tracked and exit objects. For object entrance, queries (object "3") in q_{en}^i with track scores higher than the entrance threshold τ_{en} are kept while the left queries are removed:

$$\tilde{q}_{en}^i = \{q_k \in q_{en}^i | s_k > \tau_{en}\} \quad (2)$$

where s_k is the classification score corresponding to the k^{th} query q_k in q_{en}^i . For object exit process, queries (object "2") in q_{ce}^i with track scores lower than the exit threshold τ_{ex} for consecutive M frames is removed and the queries left (object "1") will be kept:

$$\tilde{q}_c^i = \{q_k \in q_{ce}^i | \max\{s_k^i, \dots, s_k^{i-M}\} > \tau_{ex}\} \quad (3)$$

In practice we set $\tau_{en} = 0.8$, $\tau_{ex} = 0.6$ and $M = 5$.

Temporal Aggregation Network: In the last section, we introduce the object entrance and exit mechanism to deal with the entrance and exit objects. In this section, we introduce the temporal aggregation network (TAN) to enhance the temporal relation and provide contextual priors for the tracked objects. As shown in Fig. 4, we first build up the so-called query memory bank for the temporal aggregation of tracked objects. The memory bank $q_{bank} = \{\tilde{q}_c^{i-M}, \dots, \tilde{q}_c^i\}$ firstly collects the queries in history that corresponds to the tracked objects. Then the queries in the memory bank will be concatenated together:

$$tgt = \tilde{q}_c^{i-M} \oplus \dots \oplus \tilde{q}_c^{i-1} \oplus \tilde{q}_c^i \quad (4)$$

The concatenated queries are input to the multi-head attention (MHA) module as both the value and key element

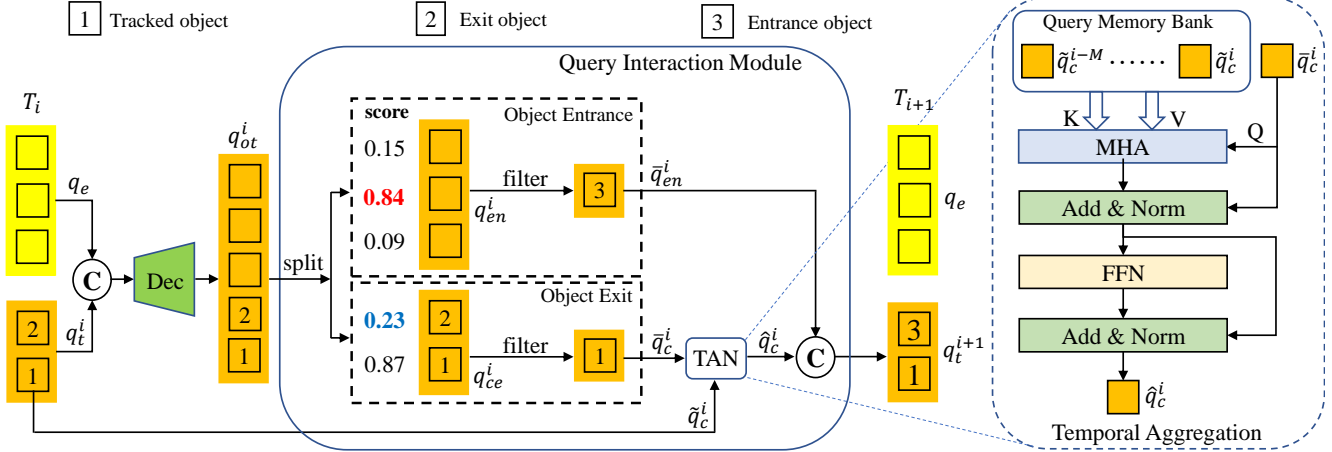


Figure 4. The process of the query interaction module (QIM) in detail. For the T_i frame, the original track query q_{ot}^i generated by the decoder from the last frame is split into two parts: one is for the object entrance (entrance query) and another one is for the object exit (exit query). The query in entrance query whose score is higher than the given entrance score is kept while the left is removed. The query in the exit query whose score is lower than the given exit score is removed.

to generate the attention weights. \bar{q}_c^i is treated as the query element of MHA and updated by dot production:

$$q_{sa}^i = \sigma_s\left(\frac{tgt \cdot tgt^T}{\sqrt{d}}\right) \cdot \bar{q}_c^i \quad (5)$$

where σ_s is the softmax function and d is the dimension of track query. After that, the q_{sa}^i is further refined by a feed forward neural network (FFN):

$$\tilde{tgt} = LN(q_{sa}^i + \bar{q}_c^i) \quad (6)$$

$$\hat{q}_c^i = LN(FC(\sigma_r(FC(\tilde{tgt})) + \tilde{tgt})) \quad (7)$$

where FC denotes a linear projection layer and LN is the layer normalization. σ_r is the ReLU activation function. The output \hat{q}_c^i of TAN is concatenated with \bar{q}_{en}^i to produce the track query set q_t^{i+1} for the T_{i+1} frame.

3.2.3 Overall Optimization

In this section, we describe the training process of MOTR in detail. Given a video sequence as the input, our training loss, namely track loss, is calculated frame-by-frame along with the frame-by-frame generated predictions. The overall track loss is the sum of track losses of all frames normalized by the number of all GTs over the training samples:

$$L_{ot}(Y, \hat{Y}) = \frac{\sum_{n=0}^N (L_t(Y_i, \hat{Y}_i))}{\sum_{n=0}^N (V_i)} \quad (8)$$

where N is the length of video sequence. Y_i and \hat{Y}_i are the predictions and the matched GTs at T_i frame, respectively. $V_i = V_t^i + V_e^i$ denotes the total number of GTs at

T_i frame. V_t^i and V_e^i are the numbers of tracked objects and new tracks, respectively. L_t is the track loss of single frame, which is similar to the detection loss in Deformable-DETR. The track loss for the single-frame image L_t can be formulated as:

$$L_t(Y_i, \hat{Y}_i) = \lambda_{cls} L_{cls} + \lambda_{l_1} L_{l_1} + \lambda_{giou} L_{giou} \quad (9)$$

where L_{cls} is focal loss [19]. L_{l_1} denotes L1 loss and L_{giou} is the generalized IoU loss [29]. λ_{cls} , λ_{l_1} and λ_{giou} are the corresponding weight coefficients.

The main difference between our track loss and the detection loss in Deformable-DETR is the label assignment (how to assign the GTs to each prediction as the supervision). For the detection loss, the label assignment is fully determined by the Hungarian Matching between all GTs and predictions. While for our track loss, since the track query is responsible to predict for the specific object it tracks (As discussed in Sec. 3.2.1), the GT object of a track query is determined by the identity of the object the query tracks. As for the empty query, GT object of its prediction is determined by Hungarian Matching between the prediction of empty query and the GTs of new tracks.

4. Experiments

4.1. Datasets and Metrics

Datasets: MOT16 and MOT17 [24] contain the same video sequences, including 7 training sequences and 7 test sequences. The main difference between them is the detection ground-truth labels. In public detection, detection inputs of MOT16 are obtained by the DPM [11] detector while that of MOT17 are generated by DPM, Faster R-CNN [28] and SDP [42] object detectors.

Dataset	Tracker	Public Detection	MOTA↑	IDF1↑	MT (%) ↑	ML (%)↓	FP↓	FN↓	IDS↓
MOT16	FWT[13]	✓	47.8	44.3	19.1	38.2	8886	85487	852
	MOTDT[9]	✓	47.6	50.9	15.2	38.3	9253	85431	792
	GCRA[21]	✓	48.2	48.6	12.9	41.1	5104	88586	821
	EAMTT[30]		52.5	53.3	19.0	34.9	4407	81223	910
	Tracktor++[1]	✓	54.4	52.5	19.0	36.9	3280	79149	682
	SORTwHPD16[2]		59.8	53.8	25.4	22.7	8698	63245	1423
	smartSORT[23]		60.4	56.1	28.9	21.2	11183	59867	1135
	DeepSORT_2[41]		61.4	62.2	32.8	18.2	12852	56668	781
	JDE[39]		64.4	55.8	35.4	20.0	/	/	1544
	MOTR (Ours)		65.7	67.0	37.2	20.9	16512	45340	648
MOTR (Ours)	✓	65.8	67.1	32.5	27.4	9914	51965	547	
MOT17	MHT DAM[14]	✓	50.7	47.2	20.8	36.9	22875	252889	2314
	MOTDT17[9]	✓	50.9	52.7	17.5	35.7	24069	250768	2474
	FWT[13]	✓	51.3	47.6	21.4	35.2	24101	247921	2648
	SST[36]		52.4	49.5	21.4	30.7	25423	234592	8431
	Tracktor++[1]	✓	53.5	52.3	19.5	36.6	12201	248047	2072
	Tracktor v2[1]	✓	56.5	55.1	21.1	35.3	8866	235449	3763
	CenterTrack[45]	✓	61.5	59.6	26.4	31.9	14076	200672	2583
	TrackFormer [22]	✓	61.8	59.8	/	/	35226	177270	2982
	TransTrack[35]		65.8	56.9	32.2	21.8	24000	163683	5355
	CTracker[25]		66.6	57.4	32.2	24.2	22284	160491	5529
	MOTR (Ours)		65.1	66.4	33.0	25.2	45486	149307	2049
MOTR (Ours)	✓	66.5	67.0	33.5	26.2	31302	155715	1884	

Table 1. Performance comparison between MOTR and existing methods on MOT16 and MOT17 datasets under both the private and public detection protocols. On MOT16, our MOTR provides higher IDF1 scores and lower IDS compared to the state-of-the-art methods, such as JDE and DeepSORT. On MOT17, our MOTR achieves better performance than our concurrent work, TrackFormer, on both IDF1 and MOTA metrics. The number is marked in red and blue if it is the best two in the column.

Evaluation Metrics: We follow the standard evaluation protocols to evaluate our proposed method. The common metrics include Multiple-Object Tracking Accuracy (MOTA), the percentage of Mostly Tracked Trajectories (MT), Mostly Lost Trajectories (ML), Identity Switches (IDS) and Identity F1 Score (IDF1). Among these metrics, IDF1 is used to measure the trajectory identity accuracy. MOTA is the primary metric to measure the overall detection and tracking performance and it is defined as $MOTA = 1 - \frac{\sum_i FP_i + FN_i + IDSW_i}{\sum_i GT_i}$, where GT_i , FP_i , FN_i and $IDSW_i$ are the number of ground-truth bounding boxes, false positives, false negatives, and identity switches at i^{th} frame, respectively.

4.2. Implementation Details

Following the settings in CenterTrack [45], several data augmentation methods, such as random flip and random crop, are adopted. The shorter side of input images is resized to 800 and the maximum size is restricted within 1536. We randomly sample key frames from video sequences with interval to solve the problem of different frame rates. Besides, we erase the tracked queries with the probability p_{drop} to generate more samples for entrance objects and insert some false positives with the probability p_{insert} to simulate the object exit. In our experiment, p_{drop} , p_{insert} and

sampling interval are set to 0.1, 0.3 and 10, respectively.

All the experiments are conducted on PyTorch with 8 Tesla V100 GPUs. We use the Deformable-DETR [47] with ResNet50 [12] as our basic network. The basic network is pretrained on the COCO detection dataset [20]. We train our model with the AdamW optimizer for total 200 epochs with the initial learning rate of $2.0 \cdot 10^{-4}$. The learning rate decays to $2.0 \cdot 10^{-5}$ at 150 epochs. The batch size is set to 1 and each batch contains 5 frames.

For state-of-the-art comparison, we train MOTR on the joint dataset (MOT17 training set and CrowdHuman [32] val set). For the $\sim 5k$ static images in CrowdHuman val set, we apply the random shift in [45] to generate video clips with pseudo tracks. We increase the length of video clip to 3,4,5 at the 50^{th} , 90^{th} , 150^{th} epochs, respectively. The progressive increment of video clip improves the training efficiency and stability. For ablation study, we simply ignore the dataset of CrowdHuman and directly train the MOTR on MOT17 training set for 200 epochs.

4.3. State-of-the-art Comparison

As shown in Tab. 1, we compare our approach with previous methods on MOT16 and MOT17 test datasets in terms of MOTA, IDF1 and IDS metrics. MOTR achieves state-of-the-art performance on both two datasets. Our method

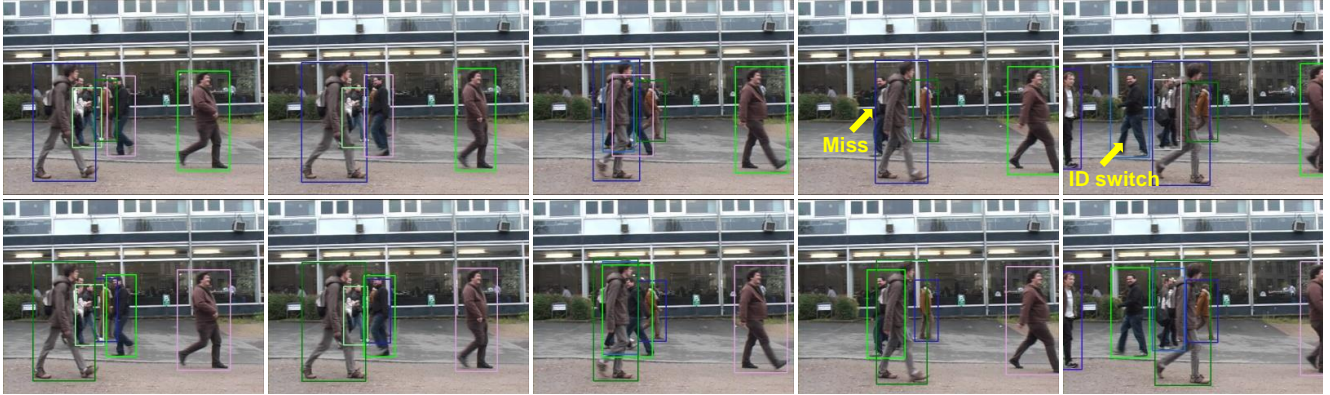


Figure 5. The effect of multi-frame continuous query passing on solving ID switch problem. When the length of video sequence is set to two (top), the objects that are occluded will miss and switch the identity. When improving the video sequence length from two to five (bottom), the track will not occur the ID switch problem with the help of enhanced temporal relation.

performs end-to-end tracking and simultaneous detection, so it does not require extra detection results as the input. However, for fair comparison, we also report the evaluation results of applying public detection to filter tracking initialization (following CenterTrack [45]) in MOTR.

In MOT16, we compare MOTR with JDE [39] and DeepSORT_2 [41], which achieve state-of-the-art performance among previous methods in MOTA and IDF1 metrics, respectively. Our method surpasses JDE by 11.3% and DeepSORT_2 by 4.9% on IDF1. Also, MOTR gets fewer IDS than JDE (547 vs. 1544) and DeepSORT_2 (547 vs. 781). As for the MOTA metric, our method also achieves better performance than JDE (65.8 vs. 64.4) and DeepSORT_2 (65.8 vs. 61.4). In MOT17, we compare our MOTR with our concurrent works, TrackFormer [22] and TransTrack [35]. Our method gets higher IDF1 scores, surpassing TransTrack by 10.1% and TrackFormer by 7.2%. It is worthy noting that MOTR produces much fewer IDS (1884 vs. 2982 and 1884 vs. 5355 compared to TrackFormer and TransTrack, respectively). For the MOTA metric, our method also achieves better performance than TransTrack (66.5 vs. 65.8) and TrackFormer (66.5 vs. 61.8).

As described in Sec. 4.1, higher IDF1 score and lower ID switches (IDS) indicate better tracking performance while higher MOTA represents the ability to detect the objects precisely. The experimental results show the effectiveness of modeling the long-range temporal relation. Though TrackFormer [22] and TransTrack [35] are also Transformer-based MOT frameworks, the temporal information is not fully explored due to the two-frame training. The lack of long-range temporal relation modeling results in relatively worse results in IDF1 and IDS metrics. It is worthy noting that our MOTR is a truly end-to-end framework for MOT without any explicit association process based on the continuous query passing mechanism. We believe that MOTR can serve as a strong baseline to be developed in the

near future.

4.4. Ablation Study

There are several critical factors in MOTR. Here, we explore how those factors influence the performance of our approach. Note that our ablation experiments are conducted using the single feature level with DC5 [47] for fast training and validated on the 2DMOT15 training dataset [17].

MOTR Components: As described in Sec. 3.2, there are two crucial components in MOTR: Temporal Aggregation Network (TAN), Multi-Frame Training (MFT). Ablation study in Tab. 2 shows the impact of integrating different components. Integrating our components to the baseline can gradually improve overall performance. Adding TAN module to the baseline improves MOTA by 7.8% and IDF1 by 13.6%. When using MFT, there are extra 8.2% and 3.7% improvements in MOTA and IDF1, respectively. It demonstrates that TAN combined with MFT can equip our method with strong temporal relation, which enhances the tracking and detection simultaneously. To better verify it, Fig. 5 visualizes the tracking results, which indicates that MFT can alleviate the problem of ID switching and object missing in occluded scenes.

TAN	MFT	MOTA \uparrow	IDF1 \uparrow	IDS \downarrow
		37.1	49.8	562
✓		44.9	63.4	257
	✓	47.5	56.1	417
✓	✓	53.1	67.1	210

Table 2. Impact of integrating our contributions into the baseline on 2DMOT15.

Video Sequence Length: The length of video sequence determines how long the continuous query passing performs. As shown in Tab. 3, we ablate the impact of video sequence length on the tracking performance. It shows that training by query passing with large video clip length can boost

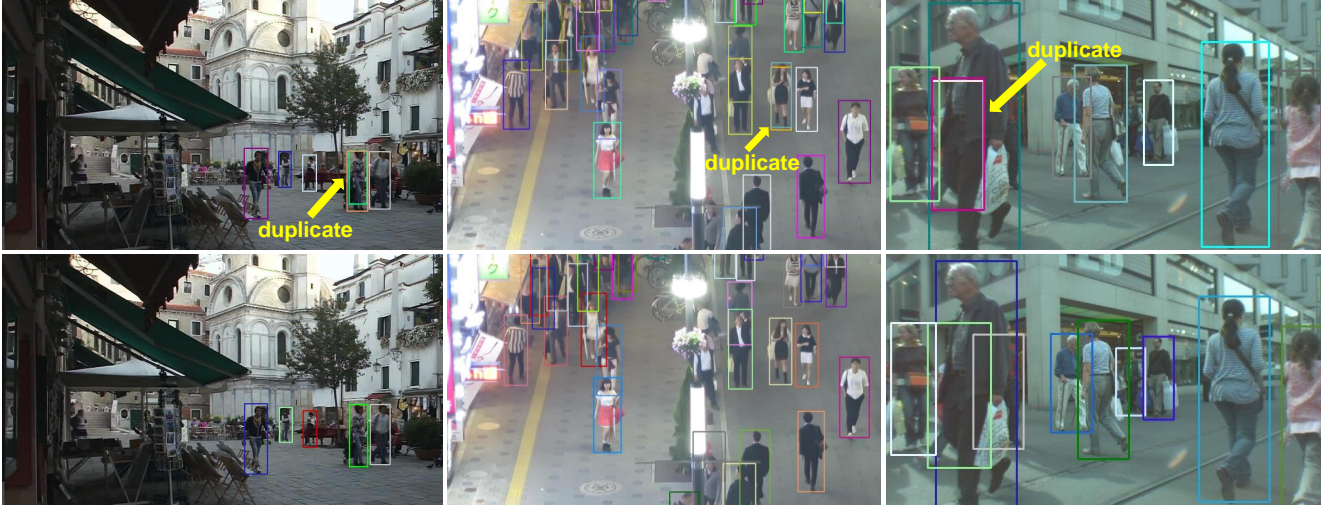


Figure 6. Comparison of tracking results regarding to the video sequence length. When the length of video sequence is set to two (top), some objects will have duplicated tracking boxes. When the video sequence length is set to five (bottom), those duplicated boxes will disappear thanks to the continuous query passing.

the tracking performance of our MOTR greatly. When the length of video clip gradually increases from 2 to 5, the MOTA and IDF1 metrics are improved by 8.2% and 3.7%, respectively. It should be noted that duplicate boxes are significantly reduced when the video clip length increases. Different from TrackFormer [22], which removes duplicate boxes by tracking NMS, our MOTR can directly produce the tracking predictions without the need for such hand-crafted operations. Please refer to Fig. 6 for comparison.

Length	MOTA \uparrow	IDF1 \uparrow	FP \downarrow	FN \downarrow	IDS \downarrow
2	44.9	63.4	16866	6649	257
3	51.6	59.4	13347	7102	424
4	50.6	64.0	13888	7104	314
5	53.1	67.1	13960	6055	210

Table 3. The impact of video sequence length on the overall tracking performance.

p_{drop}	MOTA \uparrow	IDF1 \uparrow	FP \downarrow	FN \downarrow	IDS \downarrow
0.1	53.1	67.1	13960	6055	210
0.3	51.1	69.0	14985	5926	180
0.5	48.5	62.0	15579	6356	302
0.7	41.3	54.8	16620	7935	757

Table 4. Analysis on random track query erasing.

Random Track Query Erasing: In MOT datasets, there are few cases that new objects enter in video sequences, which will do harm to the detection performance of MOTR. Erasing track queries randomly with probability p_{drop} is a good approach to simulate the entrance cases of new objects. Tab. 4 reports the performance using different value of p_{drop} during training. MOTR achieves the best performance on IDF1 and IDS when p_{drop} is set to 0.3 and best detection performance on MOTA when p_{drop} is set to 0.1. Actually,

MOTR with appropriate p_{drop} generates more samples for new objects such that the empty queries are well learned. However, too high p_{drop} may degenerate the tracking performance since the track queries are not fully trained.

Inserting Random False Positives: Similar to the new objects, there are also a small number of exit objects. During training, we sample the track queries from previous frame, whose predictions are false positives, and insert those queries into current frame to simulate the object exit cases. In Tab. 5, we explore the impact on tracking performance of setting different p_{insert} . When progressively increasing the p_{insert} from 0.1 to 0.9, our MOTR achieves the highest score in MOTA metric when the p_{insert} is set to 0.3 while the IDF1 score is continuously decreasing.

p_{insert}	MOTA \uparrow	IDF1 \uparrow	FP \downarrow	FN \downarrow	IDS \downarrow
0.1	51.2	71.7	17972	5935	148
0.3	53.1	67.1	13960	6055	210
0.5	52.1	62.0	13453	6854	345
0.7	50.7	57.7	13073	7768	444
0.9	42.3	37.2	10721	12434	1746

Table 5. The effectiveness of random false positive inserting.

5. Conclusion

We present MOTR, a truly end-to-end framework for multiple-object tracking based on recently introduced Deformable DETR. The track query is defined as each tracker and the empty query is employed to detect the new objects. Also, continuous query passing and query interaction module is introduced to enhance the temporal relation and remove the need for NMS process. The framework proposed achieves state-of-the-art performance on several MOT datasets.

References

- [1] Philipp Bergmann, Tim Meinhardt, and Laura Leal-Taixe. Tracking without bells and whistles. In *ICCV*, 2019. 1, 2, 6
- [2] Alex Bewley, Zongyuan Ge, Lionel Ott, Fabio Ramos, and Ben Upcroft. Simple online and realtime tracking. In *ICIP*, 2016. 2, 6
- [3] Erik Bochinski, Volker Eiselein, and Thomas Sikora. High-speed tracking-by-detection without using image information. In *AVSS*, 2017. 1
- [4] Erik Bochinski, Tobias Senst, and Thomas Sikora. Extending iou based multi-object tracking by visual information. In *AVSS*, 2018. 1
- [5] Necati Cihan Camgoz, Oscar Koller, Simon Hadfield, and Richard Bowden. Sign language transformers: Joint end-to-end sign language recognition and translation. In *CVPR*, 2020. 2
- [6] Nicolas Carion, Francisco Massa, Gabriel Synnaeve, Nicolas Usunier, Alexander Kirillov, and Sergey Zagoruyko. End-to-end object detection with transformers. *ECCV*, 2020. 2, 3
- [7] Xuankai Chang, Wangyou Zhang, Yanmin Qian, Jonathan Le Roux, and Shinji Watanabe. End-to-end multi-speaker speech recognition with transformer. In *ICASSP*, 2020. 2
- [8] Hanting Chen, Yunhe Wang, Tianyu Guo, Chang Xu, Yiping Deng, Zhenhua Liu, Siwei Ma, Chunjing Xu, Chao Xu, and Wen Gao. Pre-trained image processing transformer. *arXiv preprint arXiv:2012.00364*, 2020. 2
- [9] Long Chen, Haizhou Ai, Zijie Zhuang, and Chong Shang. Real-time multiple people tracking with deeply learned candidate selection and person re-identification. In *ICME*, 2018. 6
- [10] Alexey Dosovitskiy, Lucas Beyer, Alexander Kolesnikov, Dirk Weissenborn, Xiaohua Zhai, Thomas Unterthiner, Mostafa Dehghani, Matthias Minderer, Georg Heigold, Sylvain Gelly, Jakob Uszkoreit, and Neil Houlsby. An image is worth 16x16 words: Transformers for image recognition at scale. In *ICLR*, 2021. 2
- [11] Pedro F Felzenszwalb, Ross B Girshick, David McAllester, and Deva Ramanan. Object detection with discriminatively trained part-based models. *TPAMI*, 32(9):1627–1645, 2009. 5
- [12] Kaiming He, Xiangyu Zhang, Shaoqing Ren, and Jian Sun. Deep residual learning for image recognition. In *CVPR*, 2016. 3, 6
- [13] Roberto Henschel, Laura Leal-Taixé, Daniel Cremers, and Bodo Rosenhahn. Improvements to frank-wolfe optimization for multi-detector multi-object tracking. *arXiv preprint arXiv:1705.08314*, 2017. 6
- [14] Chanho Kim, Fuxin Li, Arridhana Ciptadi, and James M Rehg. Multiple hypothesis tracking revisited. In *ICCV*, 2015. 6
- [15] Harold W Kuhn. The hungarian method for the assignment problem. *Naval research logistics quarterly*, 2(1-2):83–97, 1955. 2
- [16] Laura Leal-Taixé, Cristian Canton-Ferrer, and Konrad Schindler. Learning by tracking: Siamese cnn for robust target association. In *CVPRW*, 2016. 2
- [17] Laura Leal-Taixé, Anton Milan, Ian Reid, Stefan Roth, and Konrad Schindler. Motchallenge 2015: Towards a benchmark for multi-target tracking. *arXiv preprint arXiv:1504.01942*, 2015. 7
- [18] Naihan Li, Shujie Liu, Yanqing Liu, Sheng Zhao, and Ming Liu. Neural speech synthesis with transformer network. In *AAAI*, 2019. 2
- [19] Tsung-Yi Lin, Priya Goyal, Ross Girshick, Kaiming He, and Piotr Dollár. Focal loss for dense object detection. In *ICCV*, 2017. 5
- [20] Tsung-Yi Lin, Michael Maire, Serge Belongie, James Hays, Pietro Perona, Deva Ramanan, Piotr Dollár, and C. Lawrence Zitnick. Microsoft coco: Common objects in context. In *ECCV*, 2014. 6
- [21] Cong Ma, Changshui Yang, Fan Yang, Yueqing Zhuang, Ziwei Zhang, Huizhu Jia, and Xiaodong Xie. Trajectory factory: Tracklet cleaving and re-connection by deep siamese bi-gru for multiple object tracking. In *ICME*, 2018. 6
- [22] Tim Meinhardt, Alexander Kirillov, Laura Leal-Taixe, and Christoph Feichtenhofer. Trackformer: Multi-object tracking with transformers. *arXiv preprint arXiv:2101.02702*, 2021. 2, 3, 6, 7, 8
- [23] Michel Meneses, Leonardo Matos, Bruno Prado, André de Carvalho, and Hendrik Macedo. Learning to associate detections for real-time multiple object tracking. *arXiv preprint arXiv:2007.06041*, 2020. 6
- [24] Anton Milan, Laura Leal-Taixé, Ian Reid, Stefan Roth, and Konrad Schindler. Mot16: A benchmark for multi-object tracking. *arXiv preprint arXiv:1603.00831*, 2016. 2, 5
- [25] Jinlong Peng, Changan Wang, Fangbin Wan, Yang Wu, Yabiao Wang, Ying Tai, Chengjie Wang, Jilin Li, Feiyue Huang, and Yanwei Fu. Chained-tracker: Chaining paired attentive regression results for end-to-end joint multiple-object detection and tracking. *arXiv preprint arXiv:2007.14557*, 2020. 6
- [26] Joseph Redmon and Ali Farhadi. Yolov3: An incremental improvement. *arXiv preprint arXiv:1804.02767*, 2018. 1
- [27] Shaoqing Ren, Kaiming He, Ross Girshick, and Jian Sun. Faster R-CNN: Towards real-time object detection with region proposal networks. In *NeurIPS*, 2015. 1
- [28] Shaoqing Ren, Kaiming He, Ross Girshick, and Jian Sun. Faster r-cnn: Towards real-time object detection with region proposal networks. In *NeurIPS*, 2015. 5
- [29] Hamid Rezaatoughi, Nathan Tsoi, JunYoung Gwak, Amir Sadeghian, Ian Reid, and Silvio Savarese. Generalized intersection over union: A metric and a loss for bounding box regression. In *CVPR*, 2019. 5
- [30] Ricardo Sanchez-Matilla, Fabio Poiesi, and Andrea Cavallaro. Online multi-target tracking with strong and weak detections. In *ECCV*, 2016. 6
- [31] Samuel Schulter, Paul Vernaza, Wongun Choi, and Manmohan Chandraker. Deep network flow for multi-object tracking. In *CVPR*, 2017. 2
- [32] Shuai Shao, Zijian Zhao, Boxun Li, Tete Xiao, Gang Yu, Xiangyu Zhang, and Jian Sun. Crowdhuman: A benchmark for detecting human in a crowd. *arXiv preprint arXiv:1805.00123*, 2018. 6

- [33] Sarthak Sharma, Junaid Ahmed Ansari, J Krishna Murthy, and K Madhava Krishna. Beyond pixels: Leveraging geometry and shape cues for online multi-object tracking. In *ICRA*, 2018. [2](#)
- [34] Bing Shuai, Andrew G Berneshawi, Davide Modolo, and Joseph Tighe. Multi-object tracking with siamese track-rcnn. *arXiv preprint arXiv:2004.07786*, 2020. [3](#)
- [35] Peize Sun, Yi Jiang, Rufeng Zhang, Enze Xie, Jinkun Cao, Xinting Hu, Tao Kong, Zehuan Yuan, Changhu Wang, and Ping Luo. Transtrack: Multiple-object tracking with transformer. *arXiv preprint arXiv: 2012.15460*, 2020. [2](#), [3](#), [6](#), [7](#)
- [36] ShiJie Sun, Naveed Akhtar, HuanSheng Song, Ajmal S Mian, and Mubarak Shah. Deep affinity network for multiple object tracking. *TPAMI*, 2019. [6](#)
- [37] Ashish Vaswani, Noam Shazeer, Niki Parmar, Jakob Uszkoreit, Llion Jones, Aidan N Gomez, Łukasz Kaiser, and Illia Polosukhin. Attention is all you need. In *NeurIPS*, 2017. [2](#)
- [38] Xiaolong Wang, Ross Girshick, Abhinav Gupta, and Kaiming He. Non-local neural networks. In *CVPR*, 2018. [2](#)
- [39] Zhongdao Wang, Liang Zheng, Yixuan Liu, Yali Li, and Shengjin Wang. Towards real-time multi-object tracking. In *ECCV*, 2020. [1](#), [2](#), [3](#), [6](#), [7](#)
- [40] Greg Welch, Gary Bishop, et al. An introduction to the kalman filter, 1995. [2](#)
- [41] Nicolai Wojke, Alex Bewley, and Dietrich Paulus. Simple online and realtime tracking with a deep association metric. In *ICIP*, 2017. [1](#), [2](#), [6](#), [7](#)
- [42] Fan Yang, Wongun Choi, and Yuanqing Lin. Exploit all the layers: Fast and accurate cnn object detector with scale dependent pooling and cascaded rejection classifiers. In *CVPR*, 2016. [5](#)
- [43] Dong Zhang, Hanwang Zhang, Jinhui Tang, Meng Wang, Xi-ansheng Hua, and Qianru Sun. Feature pyramid transformer. *arXiv preprint arXiv:2007.09451*, 2020. [2](#)
- [44] Yifu Zhang, Chunyu Wang, Xinggang Wang, Wenjun Zeng, and Wenyu Liu. Fairmot: On the fairness of detection and re-identification in multiple object tracking. *arXiv preprint arXiv:2004.01888*, 2020. [1](#), [2](#), [3](#)
- [45] Xingyi Zhou, Vladlen Koltun, and Philipp Krähenbühl. Tracking objects as points. *arXiv:2004.01177*, 2020. [1](#), [6](#), [7](#)
- [46] Xingyi Zhou, Dequan Wang, and Philipp Krahenbuhl. Objects as points. *arXiv preprint arXiv:1904.07850*, 2019. [1](#)
- [47] Xizhou Zhu, Weijie Su, Lewei Lu, Bin Li, Xiaogang Wang, and Jifeng Dai. Deformable detr: Deformable transformers for end-to-end object detection. In *ICLR*, 2020. [2](#), [3](#), [6](#), [7](#)